



UNIVERSITY OF LEEDS

This is a repository copy of *An experimental study of ash behaviour and the potential fate of ZnO/Zn in the Co-combustion of pulverised South African coal and waste tyre rubber*.

White Rose Research Online URL for this paper:  
<http://eprints.whiterose.ac.uk/78471/>

Version: WRRO with coversheet

---

**Article:**

Singh, S, Nimmo, W and Williams, PT (2013) An experimental study of ash behaviour and the potential fate of ZnO/Zn in the Co-combustion of pulverised South African coal and waste tyre rubber. *Fuel*, 111. 269 - 279. ISSN 0016-2361

<https://doi.org/10.1016/j.fuel.2013.04.026>

---

**Reuse**

Unless indicated otherwise, fulltext items are protected by copyright with all rights reserved. The copyright exception in section 29 of the Copyright, Designs and Patents Act 1988 allows the making of a single copy solely for the purpose of non-commercial research or private study within the limits of fair dealing. The publisher or other rights-holder may allow further reproduction and re-use of this version - refer to the White Rose Research Online record for this item. Where records identify the publisher as the copyright holder, users can verify any specific terms of use on the publisher's website.

**Takedown**

If you consider content in White Rose Research Online to be in breach of UK law, please notify us by emailing [eprints@whiterose.ac.uk](mailto:eprints@whiterose.ac.uk) including the URL of the record and the reason for the withdrawal request.



[eprints@whiterose.ac.uk](mailto:eprints@whiterose.ac.uk)  
<https://eprints.whiterose.ac.uk/>

*promoting access to White Rose research papers*



**Universities of Leeds, Sheffield and York**  
**<http://eprints.whiterose.ac.uk/>**

---

This is an author produced version of a paper published in **Fuel**.  
White Rose Research Online URL for this paper:

<http://eprints.whiterose.ac.uk/78471/>

---

**Paper:**

Singh, S, Nimmo, W and Williams, PT (2013) *An experimental study of ash behaviour and the potential fate of ZnO/Zn in the Co-combustion of pulverised South African coal and waste tyre rubber*. Fuel, 111. 269 – 279.

<http://dx.doi.org/10.1016/j.fuel.2013.04.026>

---

# An Experimental Study of Ash Behaviour and the Potential Fate of ZnO/Zn in the Co-Combustion of Pulverised South African Coal and Waste Tyre Rubber

S. Singh\*, W. Nimmo and P.T. Williams

Energy Research Institute (ERI), Energy Building, The University of Leeds, LS2 9JT, UK

## Abstract

A Novel combustion application utilising waste tyre rubber (WTR) as a secondary fuel in pulverised coal power plants is presented. Co-combustion of a South African coal (SAf) with WTR at the fuel fractions (FF) 4.1%, 14.1% and 19.7% along with the pure firing of WTR was conducted in an 80 kW<sub>th</sub> combustion test facility (CTF). This study assessed the potential slagging and fouling behaviour of the resultant ashes produced from co-firing SAf/WTR and pure fired WTR. XRF and ICP/OES analysis of the co-fired SAf/WTR and pure fired WTR ashes revealed a high composition of acidic oxides. Based on the fusibility indices (B/A, R<sub>s</sub>, S<sub>R</sub>, F and F<sub>u</sub>) it was determined that co-fired SAf/WTR and pure fired WTR ashes carry a low risk of slagging and fouling. ZnO is incorporated in the manufacturing of tyres as a compounding additive. ZnO is present within raw WTR, posing the question as to its fate during combustion. In this study ash collected and analysed from the pure fired WTR and co-fired SAf/WTR exhibited lower levels of Zn than anticipated. It is suggested that ZnO remains in the vapour phase within the CTF at temperatures >1200 °C. Experimental analysis found Zn enrichment at lower temperatures was not significant within the fly ash collected by the cyclone trap or ash deposits collected from the water cooled sections of the CTF. This suggests that Zn could be forming a submicron aerosol. It is further noted that ZnO/Zn is not likely to contribute significantly in the slagging/fouling mechanisms, due to its volatile nature. However this present study highlights the need for further experimental assessment of co-firing SAf/WTR required prior to any industrial application.

Keywords: Waste tyre rubber, Slagging and fouling, ZnO-Zn, Co-firing coal/waste tyre rubber.

\*Corresponding author. Tel.: +44 (0)113 343 2534

E-mail address: [s.singh@leeds.ac.uk](mailto:s.singh@leeds.ac.uk) (S. Singh)

## 1. Introduction

It is reported that approximately  $3.4 \times 10^6$  tonnes and  $4.6 \times 10^6$  tonnes of waste tyre rubber (WTR) are annually produced in Europe and the United States respectively [1]. The disposal of tyres has proved to be extremely difficult due to their highly resistant chemical, biological and physical properties. Stockpiles of waste tyres represent a serious fire hazard that can result in the exposure of pollution at high levels to the soil, atmosphere and water [2].

Fossil fuels in the form of coal, oil and gas currently provide 80% of the global energy demands [3]. Nitrogen oxide emissions (NO<sub>x</sub>) produced by pulverized coal combustors are a cause of significant environmental harm and contribute to the production of acid rain (HNO<sub>3</sub>, H<sub>2</sub>SO<sub>4</sub>) high ground level ozone (O<sub>3</sub>) concentrations, and elevated fine particulates [4, 5].

Increasingly stringent emission (SO<sub>2</sub> and NO<sub>x</sub>) control targets are being imposed in Europe by the Large Combustion Plant Directive (LCPD) (2001/80/EC) for combustion plants greater than 50 MW. The target for NO<sub>x</sub> emissions has been set for 200 mg/m<sup>3</sup> by 2016. To achieve this target, power stations will be required to implement additional secondary measures (SCR, SNCR, absorption of NO<sub>x</sub> and flue gas recycle) to complement existing primary measures such as fuel-staging (reburning), Air-staging, Low-NO<sub>x</sub> burner technology, flue gas recirculation and high temperature NO<sub>x</sub> reduction [6].

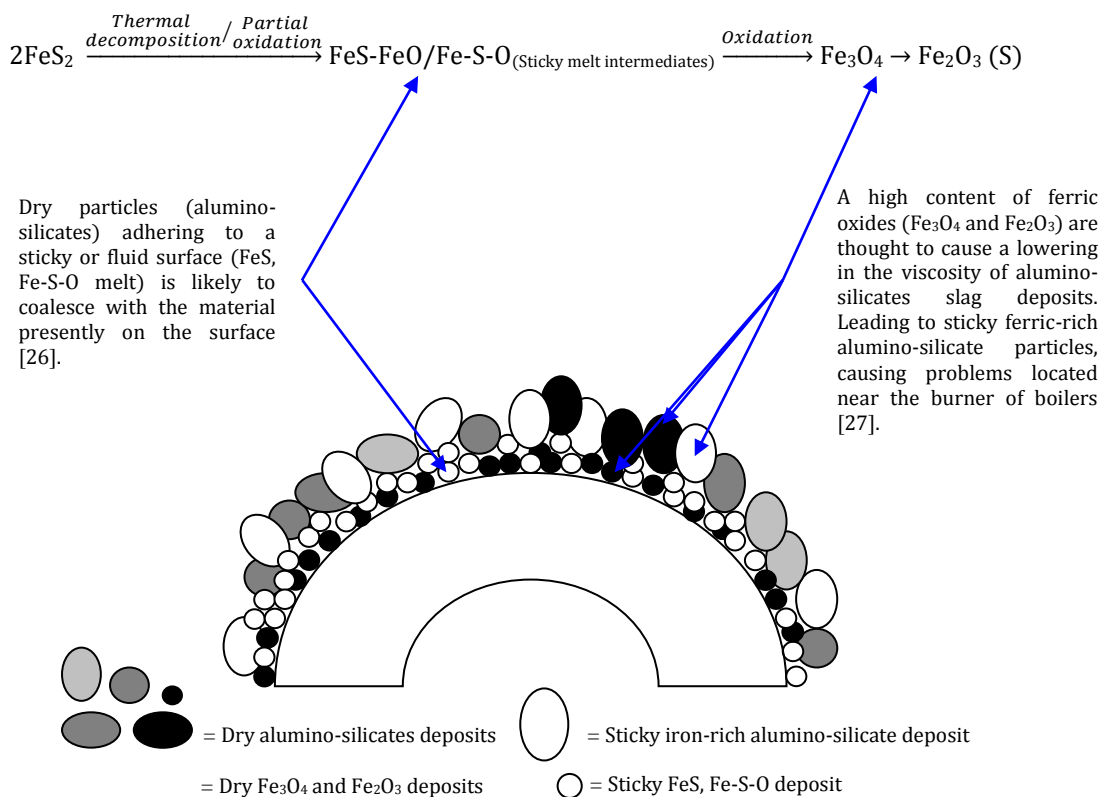
Emerging novel applications of co-firing technologies using waste tyre rubber under air firing and air staged conditions has the potential to reduce NO<sub>x</sub> emissions and utilise a waste stream in one process [7-9]. WTR demonstrates a previously overlooked source of energy for coal fired power plants. WTR is an ideal source of hydrocarbon radicals possessing a low nitrogen content, low chlorine content, and a high calorific value of approximately 38 MJ/kg (Gross)[10-13].

Emission of trace elements (toxic heavy metals) from combustion sources is undesirable due to the associated health effects [14]. Combustion of WTR within a coal fired plant may present a challenge due to its respective zinc (Zn) content. Zn in the form of zinc oxide (ZnO) is a catalyst and compounding additive used to aid in the vulcanisation process of tyre manufacture. The ZnO wt% within tyres can range from 2-4 wt% [15,16], on combustion the ZnO will significantly concentrate within the ash. Therefore it is important to examine the partitioning behaviour of ZnO/Zn between the condensed (bottom-ash and fly ash) and vapour phases (sub-micron aerosol) within a combustion test facility (CTF).

### 1.2 Slagging mechanism

The melting of inorganic minerals ( $\text{SiO}_2$ ,  $\text{Al}_2\text{O}_3$ ,  $\text{Fe}_2\text{O}_3$ ,  $\text{CaO}$ ,  $\text{MgO}$ ,  $\text{Na}_2\text{O}$  and  $\text{K}_2\text{O}$ ) present within coal can form a liquid phase (slag-melt). This slag-melt is responsible for the most severe ash deposition related problems encountered within a boiler. Slagging and fouling of the heat transfer surfaces effectively limits the load of electrical generation [17, 18]. Experimental studies [19-23] have revealed that slag formation is due initially to the formation of an iron rich layer. It is further mentioned that the iron in coal is predominantly derived from the mineral pyrite ( $\text{FeS}_2$ ) [23]. The pyrite ( $\text{FeS}_2$ ) present within the mineral matter of coal undergoes thermal decomposition to pyrrhotite ( $\text{FeS}$ ). The resultant oxidation of the pyrrhotite creates a sticky molten iron sulphide ( $\text{FeS-FeO/Fe-S-O}$ ) [24]. It is the sticky particles that deposit on clean surfaces, as they stick, a dry deposited layer forms ( $\text{Fe}_2\text{O}_3$ ). Build-up of this deposited layer increases the surface temperature and some particles can remain sticky. Impaction of dry particles to this sticky layer is instrumental in slag formation. It is further noted that the dry deposited layer of  $\text{Fe}_2\text{O}_3$  can act as a fluxing agent with aluminosilicates forming iron-rich aluminosilicates, having a reduced viscosity and increased adhesion properties (Fig 1) [25].

**Fig 1.** Impaction mechanism of coarse ash particles on a radiant heat transfer surface.



### 1.3 Fouling mechanism

Post combustion problems associated with mineral matter can be as troublesome as slag formation during combustion. Mineral matter in the form of vaporised trace elements typically high in alkali and earth metals ( $\text{Ca}$ ,  $\text{Na}$ ,  $\text{K}$ , and  $\text{Mg}$ ) are known to condense on the cooler regions of a boiler, mainly the convective heat transfer sections [27-29] (Fig 2). These trace elements are known to form vapour phase sulphates that are able to condense onto cooler surfaces. As the deposits increase in thickness, a resultant fused mass with insulating properties increases the surface temperature. This insulation effect leads to the formation of the sticky layer. The build-up of deposits onto the sticky layer can be rapid and occur in the direction of the flue gas flow as non-sticking ash particles adhere to this surface via the mechanism of impaction (Fig 2) [26].

**Fig 2.** Potential fouling mechanisms on convective heat exchange surfaces.

Researchers [27-30] state that potential slagging and fouling problems are due to the operating conditions of coal fired boilers, along with the quantities of mineral matter present within coal. These factors are reported as dictating how the mineral matter behaves during combustion and also post combustion. Fusibility correlations have been developed in order to assess the propensity for possible slagging and fouling that may arise within the combustion zone and post-combustion sections. Table 1 summarises the fusibility correlations widely used for coal and biomass co-firing [30, 31].

**Table 1**  
Slagging and fouling fusibility correlations [30, 31].

Fusibility Correlations		Low	Medium	High	Severe
$\frac{B}{A} = \left( \frac{Fe_2O_3 + CaO + Na_2O + K_2O + MgO}{SiO_2 + Al_2O_3 + TiO_2} \right)$	EQ-1	<0.6	0.6-2.0	2.0-2.6	>2.6
Slagging (Babcock)Rs = $\left( \frac{B}{A} \right) \times S^{daf}$	EQ-2	<0.5	0.5-1.0	1.0	1.75
Ash Viscosity SR = $\left( \frac{SiO_2}{SiO_2 + Fe_2O_3 + CaO + MgO} \right)$	EQ-3	>72	$\geq 72$ $S_R > 65$	$\leq 65$	>72
Fouling Factor F = $\left( \frac{B}{A} \right) \times Na_2O$	EQ-4	<0.2	0.2-0.5	0.5-1.0	>1.0
Fouling Factor $F_u = \left( \frac{B}{A} \right) \times (K_2O + Na_2O)$	EQ-5	$F_u \leq 0.6$		$\leq 40$	$F_u > 40$

\*Let  $Fe_2O_3$ , CaO,  $Na_2O$ ,  $K_2O$  and MgO denote basic metal oxides (wt%) and let  $SiO_2 + Al_2O_3 + TiO_2$  denote acidic metal oxides (wt%) for EQ-1 to 5. Let  $S^{daf}$  = percentage of sulphur in dry fuel (EQ-3).

#### 1.4 Aim

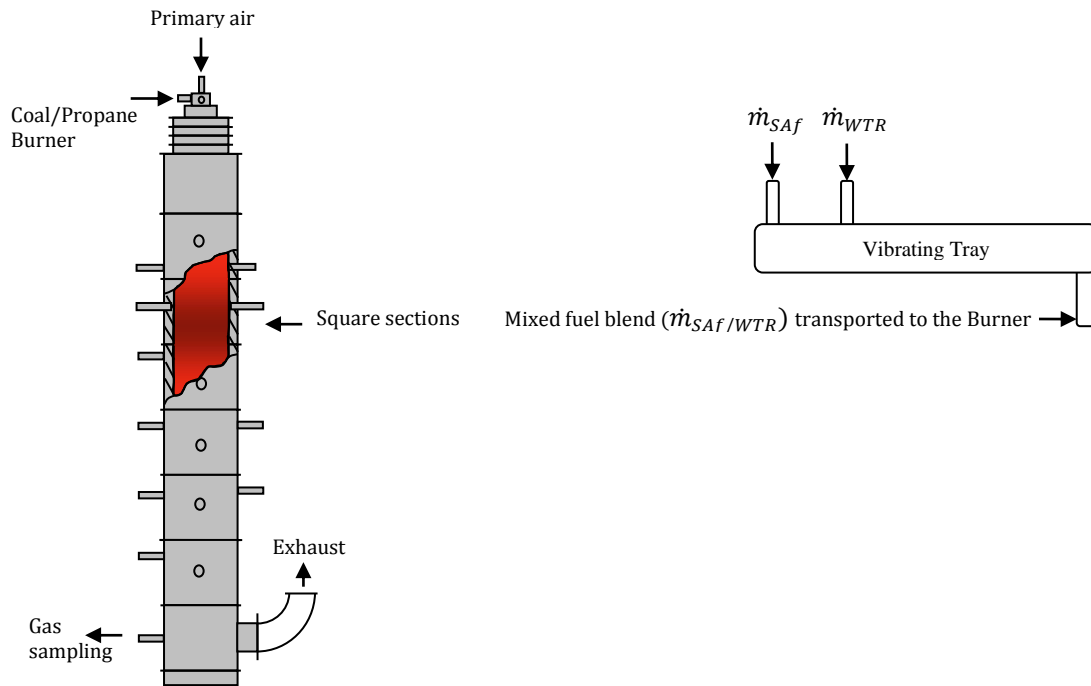
The aim of this present study is to evaluate the slagging and fouling hazard associated with the pure firing of WTR and the co-firing of South African coal/waste tyre rubber fuel blends (SAf/WTR), in comparison to that of a suite of pure fired bituminous coals, biomass and co-fired coal/biomass fuel blends. A further characterisation as to the fate of ZnO inherent within WTR, during the pure firing of WTR and the co-firing of SAf/WTR was further performed experimentally and compared to a theoretical zinc mass balance.

## 2. Experimental

### 2.1 80 kW<sub>th</sub> Combustion test facility (CTF)

Co-firing tests using a South African bituminous coal (SAf) and pulverised waste tyre rubber (WTR) were performed in a down-fired combustion test facility (CTF) operating at approximately 80 kW<sub>th</sub> (Figure 3). The overall length of the CTF is 3.5 meters consisting of square box sections with internal dimensions 350mm x 350mm. Each section is equipped with access ports to accommodate thermocouple and injection installation points. Either pulverised coal or propane (this study) could be used as the primary combustion fuel. Calibrated screw feeders (Rospen Industries Ltd) were used for feeding the primary coal feed. The WTR was supplied by SRC Ltd, UK and Charles Lawrence International (UK) in pre-sieved size ranges.

**Fig 3.** Schematic diagram of the 80 kW<sub>th</sub> combustion test facility (CTF).



## 2.2 Co-firing combustion conditions

The stoichiometry was set at  $\lambda_1 = 1.16$  (3% excess O<sub>2</sub> in the flue gas) for co-firing experiments of SAf/WTR by controlling the co-firing feed rates of the SAf and WTR. The WTR was metered via a small screw feeder and mixed with the coal flow on the spreader tray then transported pneumatically to the burner (Figure 3). Flue gas analysis was performed by drawing sample gas through appropriate sample conditioning lines to on-line gas analysis systems for O<sub>2</sub> (Servomex, paramagnetic), NO<sub>x</sub> (Signal, Chemiluminescence) and CO<sub>2</sub> and CO (ADC, NDIR). SO<sub>2</sub> (Signal) sampling was through heated sample lines (180 °C), coalescing filters and driers to avoid SO<sub>2</sub> losses. Data from the analysers and thermocouples were collected by a data-logging system (Iotech Multiscan) and stored on a PC for post-run processing and analysis. Ash particles were collected by cyclone in the flue of the combustor. The secondary fuel feed systems used for the coal and the pulverised tyre, were calibrated prior to the test runs and had a variation of approximately  $\pm 7\%$  of the feed setting. This equates to an uncertainty in the thermal fraction of waste tyre fed (FF) ranging from  $\pm 0.1$  to 1.2 %.

## 2.3 Fuel and Ash analysis

The SAf and WTR tyre analysis of CHNS and O as summarised in Table 2 has been calculated on a dry ash free basis (daf) derived from as received (ar) values.

The resultant ash produced from the pure firing of SAf and WTR along with co-firing combustion tests was captured via a cyclone trap situated upstream of the flue gas stack. Replicate samples of fly ash representative of the varying combustion conditions were collected periodically through the entire test programme. Once the CTF had sufficiently cooled ash deposited on the surfaces of the lower sections and water cooled sections was collected. The composition of the mineral matter (metal oxides) for the ashes was determined by a Spectro X-Lab 2000 energy dispersive X-ray fluorescence (XRF) and a Varian 710-ES series inductively coupled plasma-optical emission spectrometry (ICP-OES).

The ash samples generated from the pure firing of SAf, WTR and co-fired SAf/WTR fuel blends were analysed using Scanning Electron Microscopy (SEM). The system used was a Cambridge Scanning Co. Camscan Series III SEM with full computer based data handling and imaging. Particle sizing was also performed using a Malvern Mastersizer 2000 on the ashes produced from the pure firing of SAf, WTR and co-fired SAf/WTR fuel blends 4.1% FF, 14.1% FF and 19.7% FF.

The particle size distribution for pure fired SAf, WTR and co-fired SAf/WTR ashes was measured by a Malvern Mastersizer 2000.

**Table 2**

Fuel analysis and properties.

Ultimate analysis (daf, wt%)	Waste tyre rubber (WTR)	South African coal (SAf)
C	84.8	85.0
H	7.7	4.8
N	0.5	2.1
S	0.9	0.7
O	6.4	7.2
Proximate analysis (wt%)		
M	0.2	2.9
V	65.4	24.7
FC	26.1	56.7
A	8.1	15.7
XRF/ICP-OES analysis ZnO (wt%)	2.6	0.07

#### 2.4 Mass balance

A mass balance based on the theoretical content (wt%) of ZnO within the pure fired SAf, WTR and the co-fired SAf/WTR fuel blends was determined and compared to the measured values of ZnO wt%. In order to validate the mass balance methodology employed, a comparison between theoretical and measured values for SiO<sub>2</sub> wt% was performed. SiO<sub>2</sub> is a significant mineral constituent of coal and tyre ash [15, 19-30]. The experimental uncertainty between the theoretical mass balance and measured values ranges from  $\pm 1.2\%$  to 9.8% (Table 3). The experimental uncertainty of  $\pm 1.2\%$  to 9.8% between the theoretical and measured values of SiO<sub>2</sub> is within an acceptable range, further validating the mass balance methodology employed to determine the theoretical wt% of ZnO.

### 3. Results and discussions

#### 3.1 Comparison of predicted ash deposition behaviour between a suite of coals, biomass, WTR and co-fired SAf/WTR fuel blends.

A comparison of the ash deposition behaviour for SAf coal used in this present study was compared to historical co-combustion studies using an Upper Silesian bituminous coal (USi) [31], Canadian high sulphur bituminous coal (CAn) [32] and a German bituminous coal (GEr) [33] (Table 3). A low slagging potential according to the B/A (EQ-1) and Babcock slagging ( $R_s$ ) (EQ-2) index is predicted for the SAf and GEr coals (Table 3). In comparison the CAn and USi coals provide a medium to high risk of slagging (B/A,  $R_s$ ). It is noted that the  $R_s$  index incorporates the percentage of sulphur in dry fuel. Sulphur in the form of FeS<sub>2</sub> can alter the oxidation state of iron having a direct impact on slagging behaviour [20]. Oxidation of the initial sticky pyrite intermediates (FeS-FeO) to Fe<sub>3</sub>O<sub>4</sub> and Fe<sub>2</sub>O<sub>3</sub> act as a fluxing agent for highly viscous glassy phase aluminosilicates. This lowers the viscosity and temperature at which a significantly less viscous slag melt is formed. It is further noted that compositions of Fe<sub>2</sub>O<sub>3</sub> > 10 wt% increase the slagging risk as the ash viscosities can be lowered significantly [25, 34]. This would explain why the GEr, CAn and USi coals all exhibit medium and high slagging potentials, characterised by their respective ash viscosities ( $S_R$ , EQ-3). Their respective contents of Fe<sub>2</sub>O<sub>3</sub> are 10.1 wt%, 36 wt% and 12.2 wt% all >SAf (3.7 wt%) coal (Table 4).

**Table 4**  
 Pure fired fuel ashes represented by their respective mineral matter as major metal oxides (ash oxide analysis  $Me_xO_y$  in wt%), sulphur content on a dry ash free basis (daf%) and predicted slagging and fouling behaviour based on fusibility indices (Table 1).

$Me_xO_y$ (wt%)	Present Study South African coal (SAF)	[31] Upper Silesian coal (USi)	[32] Canadian high sulphur bituminous coal (CAAn)	[33] German bituminous coal (GEr)	Present study Waste tyre rubber (WTR)	[31] Wood (WD)	[31] Straw (ST)	[31] Sewage sludge (SS)	[31] Bone Meal (BM)	[32] Wood (WD)	[33] Straw (ST)
$Al_2O_3$	31.0	10.2	19.0	28.3	17.2	8.4	0.3	9	0	3.2	0.6
CaO	8.1	15.1	5.0	5.3	1.31	56.7	8.1	13.9	18.81	6	9.7
$Fe_2O_3$	3.7	12.2	36.0	10.1	2.31	3.6	0.2	24.6	0.85	1.5	1.2
$K_2O$	0.6	2.5	1.4	3.6	2.22	5.3	32	2.2	1.12	14	18.5
MgO	1.4	4.9	0.9	2.8	0.78	9.5	7.2	2.8	0.27	1.4	1.8
$Na_2O$	0.1	1.0	0.8	1.2	0.75	3.2	0.5	4.9	2.94	0.92	0.2
$P_2O_5$	1.8	0.1	0.7	0.5	0.56	4.7	1.5	19.3	70.1	2.8	2.3
$SiO_2$	49.1	53.7	28.0	44.2	57.3	8.5	50	22.4	5.96	58	67
$TiO_2$	1.9	0.3	0	1.1	0.82	0.1	0.2	0.9	0	0	0.1
ZnO	0	0	0	0	20.16	0	0	0	0	0	0
*Other	1.6	0.1	8.3	1.6	0	8.4	0.3	0	0	5.4	0
Total	100	100	100	100	100	100	100	100	100	100	100
$S^{daf}$	0.7	1.2	2.4	1.1	0.9	0	0	1.1	1	0.12	0.31
Indices											
$\frac{B}{A}$	0.17	0.55	0.94	0.31	0.10	4.61	0.95	1.50	4.03	0.39	0.46
$R_s$	0.12	0.67	2.25	0.35	0.26	4.61	0.95	1.65	4.03	0.05	0.14
$S_R$	78.89	62.56	40.07	70.83	92.87	10.86	76.34	35.16	23.02	86.70	84.07
F	0.02	0.54	0.71	0.38	0.07	14.74	0.48	7.34	11.83	0.36	0.09
$F_u$	0.13	1.93	1.99	1.50	0.29	39.15	30.89	10.64	16.34	5.81	8.67
Basic $Me_xO_y$	13.9	35.6	44.0	23	7.37	78.3	48.0	48.4	94.0	23.8	31.4
Acidic $Me_xO_y$	82.0	64.2	47.7	73.6	75.32	17.0	50.5	32.3	6.0	61.2	67.7

\*Other =  $Me_xO_y$  that are not included in the fusibility correlations but were identified as part of the mineral matter matrix by x-ray fluorescence (XRF) and inductively coupled plasma optical emission spectrometry (ICP-OES). They are included as being  $Ga_2O_3$ , Se, Br,  $Rb_2O$ , SrO,  $Y_2O_3$ , ZrO<sub>2</sub>,  $Nb_2O_5$ , BaO, PbO, ThO<sub>2</sub>,  $V_2O_5$ ,  $Cr_2O_3$ , MnO.

The Na<sub>2</sub>O content (0.1%) within the SAf is low therefore leading to a low fouling propensity, as predicted by the fouling factor, F (EQ-4). The GER, CAN and USi coals exhibit a similar Na<sub>2</sub>O content to the SAf, however GER, CAN and USi indicate a medium fouling factor as their B/A ratios are predicting a medium slagging potential. The fouling factor, F<sub>u</sub> (EQ-5) differs from the fouling factor, F (EQ-4) as it takes into account the sum of the K<sub>2</sub>O and Na<sub>2</sub>O content. Earlier research has demonstrated that K<sub>2</sub>O can lower ash fusion temperatures [35] at which initial deformation and softening occurs. Therefore, as a result the fouling propensity for the GER, CAN and USi increase from a medium fouling risk (EQ-4) to a high fouling hazard (EQ-5). This further demonstrates the impact K<sub>2</sub>O could have during operation of a PF boiler. In contrast the mineral matter representing WTR ash is composed heavily of acidic oxides. Consequently the slagging and fouling inclinations are all calculated to be low, further suggesting that safe operation of a PF furnace could be maintained by the introduction of tyres as a secondary fuel (Table 4).

The potential slagging hazard as indicated by the B/A, R<sub>s</sub> and S<sub>R</sub> indices (Table 1) for co-fired SAf/WTR ashes is observed to be low. The co-fired SAf/WTR fuel blends appear to carry a similar hazard for slagging to that of pure fired SAf, and GER coal (Table 3 and Table 4). Further, the co-fired SAf/WTR fuel blends show a more favourable ash deposition behaviour to CAN and USi coal (Table 3). This is due to the CAN and the USi coals having their respective basic oxides in a higher ratio to their acidic oxides (Table 3). The Fe<sub>2</sub>O<sub>3</sub> content in combination with the sulphur emanating from the Canadian high sulphur bituminous coal is thought to be the mineral responsible for the creation of a potentially low viscous slag melt (Table 3). The SAf/WTR ash blends at 4.1%, 14.1% and 19.7% show significantly lower levels of Fe<sub>2</sub>O<sub>3</sub> (3.74 wt%, 3.95 wt% and 4.03 wt%). This is resultant upon both the WTR and the SAf ashes containing lower levels of ferric oxide at 2.3 wt% and 3.7 wt% respectively. The fouling hazard F and F<sub>u</sub> (EQ-4 and EQ-5) for the co-fired SAf/WTR blends is low as the Na<sub>2</sub>O and K<sub>2</sub>O are present in low quantities (Table 5).

A variety of biomass fuels investigated previously such as wood=WD, straw=ST, sewage sludge=SS and bone meal=BM [31] along with wood=WD [32] and Straw=ST [33] as co-firing fuels present unfavourable ash deposition behaviour when compared to WTR (Table 3) and co-fired SAf/WTR (Table 4). The mineral matter of WTR and ash blends of SAf/WTR are heavily composed of acidic oxides therefore the inclination of slagging and fouling is presented as being low, further suggesting that safe operation of a PF furnace could be maintained by the introduction of waste tyres as a secondary fuel. Based on the composition of the mineral matter for WD [32] and ST [33] the slagging potential is low but the fouling factor, F<sub>u</sub> is seen to be high, this is to be expected as the K<sub>2</sub>O content of the WD and ST is the highest of all the basic oxides. WD [31] displays severe slagging and fouling as CaO (56.7 wt%) an established fluxing agent of alumino-silicates, suggesting a higher proportion of sticky particles adhering to furnace water walls especially as the Al<sub>2</sub>O<sub>3</sub> and SiO<sub>2</sub> are present in low levels [25]. The high content of CaO further suggests a higher proportion of the fouling deposits being composed of sticky calcium sulphate salt (CaSO<sub>4</sub>). ST [31] provides an almost even ratio of basic oxides (48 wt%) to acidic oxides (50.5 wt%), therefore a medium slagging inclination (B/A and R<sub>s</sub>) is observed due to there being no sulphur present in the straw that could influence the oxidation state of the ferric matter [20]. The ash viscosity is high suggesting a low yield of sticky particles associated with low viscosity slag melts. The predicted fouling factor is low as the Na<sub>2</sub>O content is also low. The fouling factor F<sub>u</sub> presents a contrasting prediction attributed to the high levels of K<sub>2</sub>O. This mineral happens to be the most abundant of the basic oxides present in straw. Therefore straw presents a low risk of in furnace slag deposition but potential for significant fouling of post combustion surfaces according to the F<sub>u</sub> index. SS [31] shows a higher ratio of basic oxides (48.4 wt%) to acidic oxides (32.3 wt%) and presents a medium to high risk for slagging due to its low viscosity (S<sub>R</sub>) index, followed by a high to severe fouling as Na<sub>2</sub>O is seen to be sufficiently concentrated within the ash. BM [31] reveals a severe slagging (B/A, R<sub>s</sub> and S<sub>R</sub>) and fouling (F, F<sub>u</sub>) risk as the basic oxides are shown to be an order of magnitude 4 times greater to that of the acidic oxides (phosphorous pentoxide (P<sub>2</sub>O<sub>5</sub>) = 70 wt%). P<sub>2</sub>O<sub>5</sub> has been experimentally observed to lower the temperatures at which hemispherical deformation takes place [31].

**Table 5**

Co-fired ashes represented by their respective mineral matter as major metal oxides (ash oxides analysis  $Me_xO_y$  in wt%), sulphur content on a dry ash free basis (daf%) and predicted slagging and fouling behaviour based on fusibility indices (Table 1).

$Me_xO_y$ (wt%)	Present study SAf/WTR			[31] USi/WD				[31] USi/ST				[31] USi/SS				[31] USi/BM				[32] CA <sub>n</sub> /WD			[33] GE <sub>r</sub> /ST			
	4.1% (FF)	14.1% (FF)	19.7% (FF)	2% (FF)	5% (FF)	10% (FF)	20% (FF)	7.5% (FF)	20.3% (FF)	100% (FF)	25% (FF)	50% (FF)	100% (FF)													
Al <sub>2</sub> O <sub>3</sub>	28.35	28.88	28.28	23.33	23.16	22.87	22.22	23.31	23.11	22.76	21.97	22.15	20.53	18.43	15.57	22.92	22.16	20.89	18.39	16	12	3.2	0.6	0.21	8.29	
CaO	7.4	7.75	7.9	4.08	4.67	5.7	7.98	3.73	3.77	3.83	3.98	4.61	5.76	7.24	9.26	4.04	4.53	5.35	6.96	4.4	6	6	9.7	6.09	3.32	
Fe <sub>2</sub> O <sub>3</sub>	3.74	4.03	3.95	7.6	7.55	7.48	7.3	7.59	7.52	7.41	7.16	9.14	11.04	13.52	16.87	7.48	7.26	6.89	6.17	28	22	1.5	1.2	0	0	
K <sub>2</sub> O	0.61	0.71	0.71	2.05	2.09	2.15	2.29	2.19	2.45	2.9	3.92	2.05	2.06	2.09	2.12	2.01	1.98	1.93	1.83	3.6	6.9	14	18.5	26.07	13.7	
MgO	1.27	1.32	1.31	3.28	3.35	3.47	3.74	3.26	3.29	3.35	3.49	3.2	3.15	3.08	3	3.17	3.07	2.91	2.6	0.82	1.2	1.4	1.8	1.86	1.94	
Na <sub>2</sub> O	0.12	0.16	0.16	0.92	0.95	0.99	1.09	0.9	0.9	0.89	0.88	1.26	1.71	2.29	3.08	0.95	1.02	1.13	1.34	0.68	0.91	0.92	0.2	0.05	0.08	
P <sub>2</sub> O <sub>5</sub>	1.4	1.74	1.88	0.12	0.17	0.26	0.46	0.1	0.11	0.13	0.18	1.8	3.95	6.76	10.6	1.62	3.91	7.7	15.2	1	1.7	2.8	2.3	0	0	
SiO <sub>2</sub>	47.65	46.69	45.74	57.09	56.55	55.61	53.49	57.4	57.34	57.23	56.97	54.33	50.40	45.28	38.36	56.31	54.63	51.85	46.36	38	38	58	67	53.01	40.97	
TiO <sub>2</sub>	1.62	1.76	1.69	1.52	1.5	1.47	1.41	1.52	1.51	1.49	1.44	1.47	1.4	1.31	0	1.49	1.44	1.36	1.20	0	0	0	0.1	0	0	
ZnO	0.32	0.65	0.82	0	0	0	0	0	0	0	0	0	0	0	0	0	0	0	0	0	0	0	0.1	0.03	2.1	
*Other	6.9	5.6	6.9	0	0	0	0	0	0	0	0	0	0	0	0	0	0	0	7.5	11.3	12.2		5.8	23.7		
Total	100	100	100	100	100	100	100	100	100	100	100	100	100	100	100	100	100	100	100	100	100	100	100	100	100	100
S <sub>daf</sub>	0.704	0.715	0.721	0.54	0.52	0.48	0.41	0.54	0.52	0.50	0.44	0.58	0.62	0.68	0.77	0.51	0.53	0.56	0.62	1.95	1.61	0.14	0.11	0.15	0.29	
Indices																										
$\frac{B}{A}$	0.18	0.19	0.31	0.22	0.23	0.25	0.29	0.21	0.22	0.23	0.24	0.26	0.33	0.43	0.62	0.22	0.23	0.25	0.29	0.69	0.74	0.39	0.46	0.64	0.39	
R <sub>s</sub>	0.13	0.13	0.23	0.12	0.12	0.12	0.12	0.12	0.11	0.11	0.11	0.15	0.20	0.29	0.48	0.11	0.12	0.14	0.18	1.35	1.19	0.05	0.05	0.10	0.11	
S <sub>R</sub>	79.34	78.09	77.66	79.24	78.41	77.96	73.77	79.74	79.73	79.69	79.57	76.22	71.64	65.51	56.84	79.31	78.62	77.39	74.67	53.36	56.6	86.7	84.07	86.96	88.62	
F	0.022	0.030	0.050	0.201	0.218	0.245	0.317	0.193	0.197	0.201	0.213	0.327	0.561	0.994	1.918	0.208	0.233	0.278	0.68	0.47	0.674	0.36	0.00	0.032	16.72	
F <sub>u</sub>	0.13	0.16	0.27	0.65	0.65	0.70	0.78	0.98	0.66	0.73	0.85	1.16	0.86	1.24	1.90	3.24	0.65	0.68	0.75	2.97	5.78	5.81	8.67	16.72	5.33	
Basic Me <sub>x</sub> O <sub>y</sub>	13.14	13.97	14.04	17.93	18.61	19.79	22.40	17.67	17.93	18.38	19.43	20.26	23.72	28.22	34.33	17.65	17.86	18.21	18.90	37.50	37.01	23.82	31.40	34.07	19.04	
Acidic Me <sub>x</sub> O <sub>y</sub>	77.62	77.33	75.71	81.94	81.21	79.95	77.12	82.23	81.96	81.48	80.38	77.95	72.33	65.02	55.12	80.72	78.23	74.10	65.95	54.00	50.00	61.20	67.70	53.22	49.26	

\*Other = Me<sub>x</sub>O<sub>y</sub> that are not included in the fusibility correlations but were identified as part of the mineral matter matrix by x-ray fluorescence (XRF) and inductively coupled plasma optical emission spectrometry (ICP-OES). They are included as being Ga<sub>2</sub>O<sub>3</sub>, Se, Br, Rb<sub>2</sub>O, SrO, Y<sub>2</sub>O<sub>3</sub>, ZrO<sub>2</sub>, Nb<sub>2</sub>O<sub>5</sub>, BaO, PbO, ThO<sub>2</sub>, V<sub>2</sub>O<sub>5</sub>, Cr<sub>2</sub>O<sub>3</sub>, MnO.

### *3.2 Predicted slagging and fouling deposition behaviour for co-fired SAf/WTR ashes in comparison to co-fired coal/biomass ashes.*

The co-fired SAf/WTR ashes resultant from the fuel blends 4.1%, 14.1% and 19.7% are presented in Table 4. It is observed that the ratio of basic to acidic oxides for the co-fired SAf/WTR ashes are similar in comparison to SAf ash (pure fired SAf) (Table 4). The SAf ash has already demonstrated a low slagging hazard according to the  $R_s$ , B/A and  $S_R$  indices (Table 1) along with a low fouling ( $F$ ,  $F_u$ ) hazard. The co-fired SAf/WTR ashes for the fuel fractions 4.1%, 14.1% and 19.7% appear to follow this trend, as the  $Fe_2O_3$  and CaO are in a similar wt% to the pure fired SAf coal ash (Table 4). Based on the fusibility correlations detailed in Table 1, co-fired SAf/WTR fuel blend ashes seem to pose no more of a slagging or fouling hazard than the pure firing of SAf coal.

In the co-fired GER/ST study [33] a similarly low slagging probability to co-fired SAf/WTR is shown along with a low fouling potential,  $F$ . However a high fouling factor,  $F_u$  is predicted as the  $K_2O$  content is significantly high. This further suggests that sufficient dilution of the  $K_2O$  that is significantly inherent within the straw is not occurring when co-firing takes place with GER coal. The  $K_2O$  content in SAf/WTR ashes is significantly lower in comparison (Table 5).

Co-firing SAf/WTR further shows a more favourable ash deposition behaviour compared to co-fired CAN/WD [32] which ranges from severe to medium (Table 5). The ferric oxide in combination with the sulphur emanating mainly from the Can coal as opposed to the WD is thought to be the mineral responsible for the creation of a potentially low viscous slag melt (Table 3 and Table 4). In contrast SAf/WTR ashes from the fuel blends of 4.1%, 14.1% and 19.7% showed significantly lower levels of ferric oxide (3.74 wt%, 3.95 wt% and 4.03 wt% respectively). This is resultant upon both the pure WTR and the pure SAf ashes containing inherently low levels of ferric oxide at (2.3 wt% and 3.7 wt% respectively). The fouling hazard,  $F_u$  for the co-fired CAN/WD is due to the high inherent  $K_2O$  within the WD [31].

The ashes emanating from the previous co-fired study of USi/ST and USi/BM FF (2%, 5%, 10% and 20%) [31] exhibit a low slagging hazard, much like SAf/WTR ashes derived from the co-fired fuel fractions of 4.1%, 14.1% and 19.7%. This may be due in part to the basic oxides being in a much lower ratio to the acidic oxides (Table 4). The USi/SS [31] does deviate from this trend as the ferric oxide is seen to increase with higher fuel fractions and so predicting a medium to high slag melt corresponding to ashes with significantly less viscous properties (Table 5).

Therefore the SAf/WTR ashes present a low risk of slag formation much like some of the co-fired biomasses investigated [31-33]. The same cannot be said for the fouling risk of the co-fired biomasses [31-33]. A high fouling hazard according to the  $F_u$  (EQ-5) is likely, as  $K_2O$  for the biomasses ranges from 1.4 wt% to 26.1 wt%. The behaviour of the ash blends for co-fired SAf/WTR in comparison to the co-fired biomass studies indicates a far lower fouling hazard based on the  $F_u$  index (Table 5).

### *3.3 Fate of ZnO-Zn for pure fired WTR and co-fired SAf/WTR fuel blends*

XRF analysis of the SAf/WTR ashes measured a ZnO wt% of 0.29, 0.62 and 0.74 for the following SAf/WTR fuel blends 4.1%, 14.1% and 19.7% respectively (Table 6). The SAf/WTR ashes were collected by a cyclone trap located above the second cooling section of the CTF exhaust flue. The expected ZnO wt% within the ashes according to a predicted ZnO mass balance should be ~2.19 wt%, ~4.83 wt% and ~6.28 wt% for the SAf/WTR fuel blends of 4.1%, 14.1% and 19.7% respectively (Table 6, Appendix). The difference between the actual and predicted ZnO wt% are in the following orders of magnitude 7.5, 7.8 and 8.5 respectively. Tyres typically contain between 2 wt% to 2.5 wt% [15], hence the corresponding ZnO wt% within the tyre ash alone should equate between ~20 wt% to ~25 wt%, under normal ashing techniques employed. The XRF analysis of the raw WTR ashed within a temperature controlled furnace measured 19.6 wt% ZnO (Table 5). In contrast XRF/ICP-OES analysis of the pure fired tyre ash generated within the CTF revealed a ZnO wt% of 8.8. This is significantly lower than that measured in the raw tyre ash (19.6 wt%) approximating to a loss of 55% in the ZnO wt%. It is anticipated that dilution of the ZnO would occur due to the mixing of the WTR and the low levels of ZnO present in the SAf coal (Table 6), however it was not expected that dilution would be so significant. Furthermore it was not at all thought that less than half the ZnO wt% would be retained within the pure fired WTR ash residue collected from the CTF cyclone.

**Table 6**

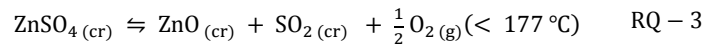
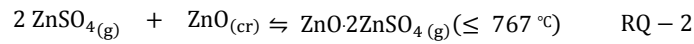
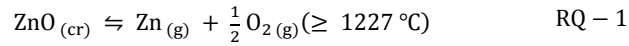
ZnO mass balance detailing the theoretical content compared to the measured content for raw WTR and the SAf/WTR ash generated from co-fired fuel blends • **4.1 FF(%)**, • **14.1 FF(%)**, and • **19.7 FF(%)** respectively.

\*Note: The measured values (▼) for the SAf/WTR ash blends • **4.1 FF(%)**, • **14.1 FF(%)**, • **19.7 FF(%)** and pure fired WTR • **100 FF(%)** SAf/WTR were determined by x-ray fluorescence (XRF) and inductively

FF(%)	$\dot{m}_{SAf}$	$\dot{m}_{WTR}$	$\dot{m}_{Ash,SAf}$	$\dot{m}_{Ash,WTR}$	$Ash_{SAf,WTR}(\%)$	$\dot{m}_{ZnO, SAf}$	$\dot{m}_{ZnO, WTR}$	$\dot{m}_{ZnO, SAf/WTR}$	$ZnO_{SAf/WTR}(\%)$	▲ Theoretical Values $ZnO_{Ash, SAf/WTR}(\%)$	▼ Measured Values $ZnO_{Ash, SAf/WTR}(\%)$
0	9.00	0.00	1.41	0.000	15.70	0.0063	0.000	0.006	0.07	1.10	-
2	8.82	0.13	1.38	0.010	15.59	0.0062	0.003	0.009	0.10	1.63	-
<b>•4.1</b>	<b>8.63</b>	<b>0.26</b>	<b>1.36</b>	<b>0.021</b>	<b>15.48</b>	<b>0.0060</b>	<b>0.007</b>	<b>0.013</b>	<b>0.14</b>	<b>2.19</b>	<b>0.29</b>
6	8.46	0.38	1.33	0.031	15.37	0.0059	0.010	0.016	0.18	2.70	-
8	8.28	0.51	1.30	0.041	15.26	0.0058	0.013	0.019	0.21	3.23	-
10	8.10	0.64	1.27	0.052	15.14	0.0057	0.016	0.022	0.25	3.75	-
12	7.92	0.77	1.24	0.062	15.03	0.0055	0.019	0.025	0.28	4.28	-
<b>•14.1</b>	<b>7.73</b>	<b>0.90</b>	<b>1.21</b>	<b>0.073</b>	<b>14.91</b>	<b>0.0054</b>	<b>0.023</b>	<b>0.028</b>	<b>0.32</b>	<b>4.83</b>	<b>0.62</b>
16	7.56	1.02	1.19	0.083	14.79	0.0053	0.026	0.031	0.36	5.32	-
18	7.38	1.15	1.16	0.093	14.67	0.0052	0.029	0.034	0.40	5.84	-
<b>•19.7</b>	<b>7.23</b>	<b>1.26</b>	<b>1.13</b>	<b>0.102</b>	<b>14.57</b>	<b>0.0051</b>	<b>0.031</b>	<b>0.037</b>	<b>0.43</b>	<b>6.28</b>	<b>0.74</b>
<b>•100</b>	<b>0</b>	<b>6.39</b>	<b>0</b>	<b>0.518</b>	<b>8.10</b>	<b>0.0000</b>	<b>0.160</b>	<b>0.160</b>	<b>2.500</b>	<b>20.25</b>	<b>8.77</b>
<b>Raw WTR</b>											<b>20.16</b>

coupled plasma-optical emission spectroscopy (ICP-OES). Refer to the Appendix for details of the mass balance determination.

The low levels of ZnO observed within the SAF/WTR ashes suggest that the Zn could be condensing out of the vapour phase onto cooler post combustion surfaces within the exhaust flue. Previous authors have noted that Zn undergoes chemical transformations within a PF boiler [36]. Transformation of most trace elements is temperature dependant,  $\geq 1227$  °C (1500 K) Zn is in a volatile gaseous state within the PF furnace [36]. Temperatures between 977-767 °C (1250 -1040 K) downstream of the burner Zn is in a crystalline form (ZnO). As the ZnO enters the exhaust flue gases at 372 °C (645 K), a crystalline oxide compound ZnO·2ZnSO<sub>4</sub> can result. The non-hydrated form of zinc sulphate (ZnSO<sub>4</sub>) is suggested to be stable between 372 -177 °C (645-450 K), temperatures below 177 °C (450 K) Zn forms a crystalline hydrated zinc sulphate (ZnSO<sub>4</sub>H<sub>2</sub>O). RQ-1 to RQ-3 summarise the higher combustion and lower post-combustion temperatures within a PF boiler [36].



\* (cr) = crystalline, (g) = gas

XRF/ICP-OES analysis of deposits taken from the water cooled sections of the CTF revealed low levels of Zn (1.0 wt% and 0.72 wt%). This suggests that Zn in the form ZnO·2ZnSO<sub>4</sub>, ZnSO<sub>4</sub> and ZnSO<sub>4</sub>H<sub>2</sub>O is not condensing on to the cooler surfaces within the exhaust flue in any significant concentration, as had been noted by [36]. It is therefore then suggested that the Zn is remaining in the flue gas and by-passing the water cooled sections and cyclone trap of the CTF. Researchers [37-41] mention trace elements that are subject to vaporisation within a PF furnace such as Zn maybe enriched within submicron particles (Fig 4). Enrichment occurs via a condensing mechanism whereby volatile species undergo heterogeneous condensation and heterogeneous nucleation. This leads to coagulation concentrated trace elements as submicron particulate matter forming an aerosol (<0.1 μm). Partitioning behaviour of trace elements can be classified into 3 broad groups (Fig 5) [42, 43]. Group 1 elements concentrate within the bottom ash and ash in equal parts. Group 2 elements of which Zn is present have been characterised as volatilising in furnace, condensing downstream within the ash or undergoing further enrichment within lower size fractions of submicron particulate matter (aerosol, <0.1 μm) [37, 42, 44 and 45]. Group 2 elements are not considered to factor significantly in the bottom ash. Group 3 represents elements that remain in the vapour phase during combustion and post combustion. It is therefore suggested that the Zn from the pure fired WTR and co-fired SAF/WTR fuel blends (4.1%, 14.1% and 19.7%) forms a submicron aerosol as opposed to enrichment within the coarse residues that make up the ash or sulphate enriched deposits suggested by previous researchers [36-41, 46 and 47]. In this aerosol phase the smaller Zn particle size and mass would by-pass the cyclone trap of the CTF. This would explain why Zn is not being enriched in the fly ash from the CTF cyclone trap as demonstrated by the XRF analysis (Table 6). Group 2 elements may either enrich sufficiently as fly ash particulate matter (<1-20 μm) or condense on the surfaces of yet finer submicron particles (<0.1 μm) [37].

**Fig 4.** Fate of trace metals during combustion in a PF furnace [47, 48].

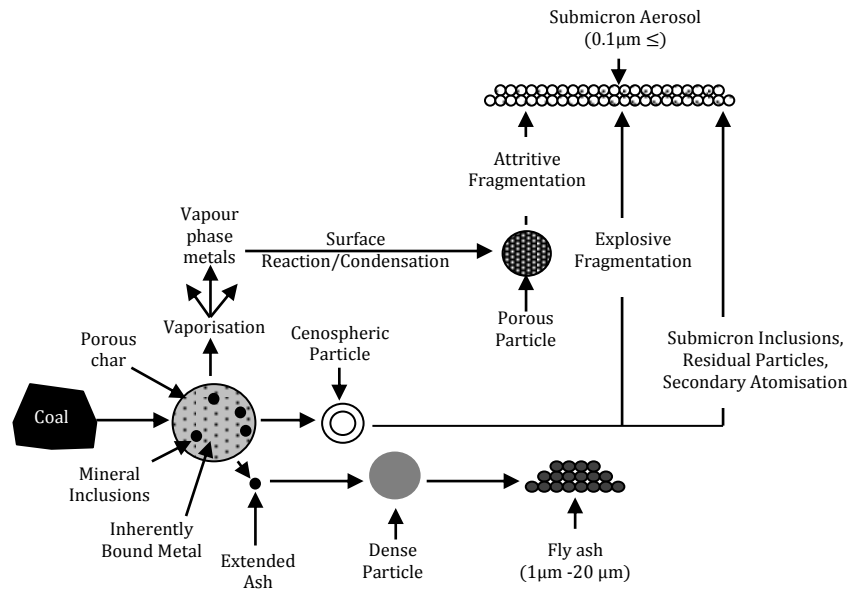


**Fig 5.** Volatility of metals categorised within a PF furnace [42, 47].

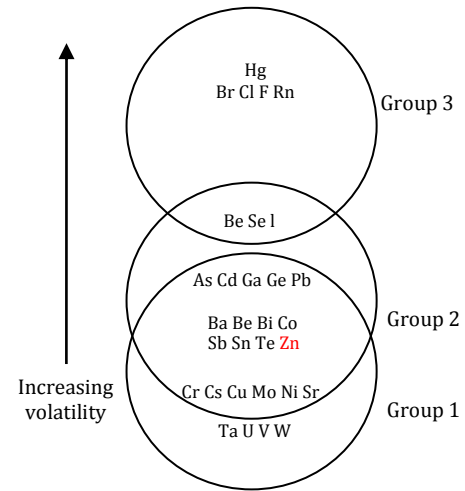
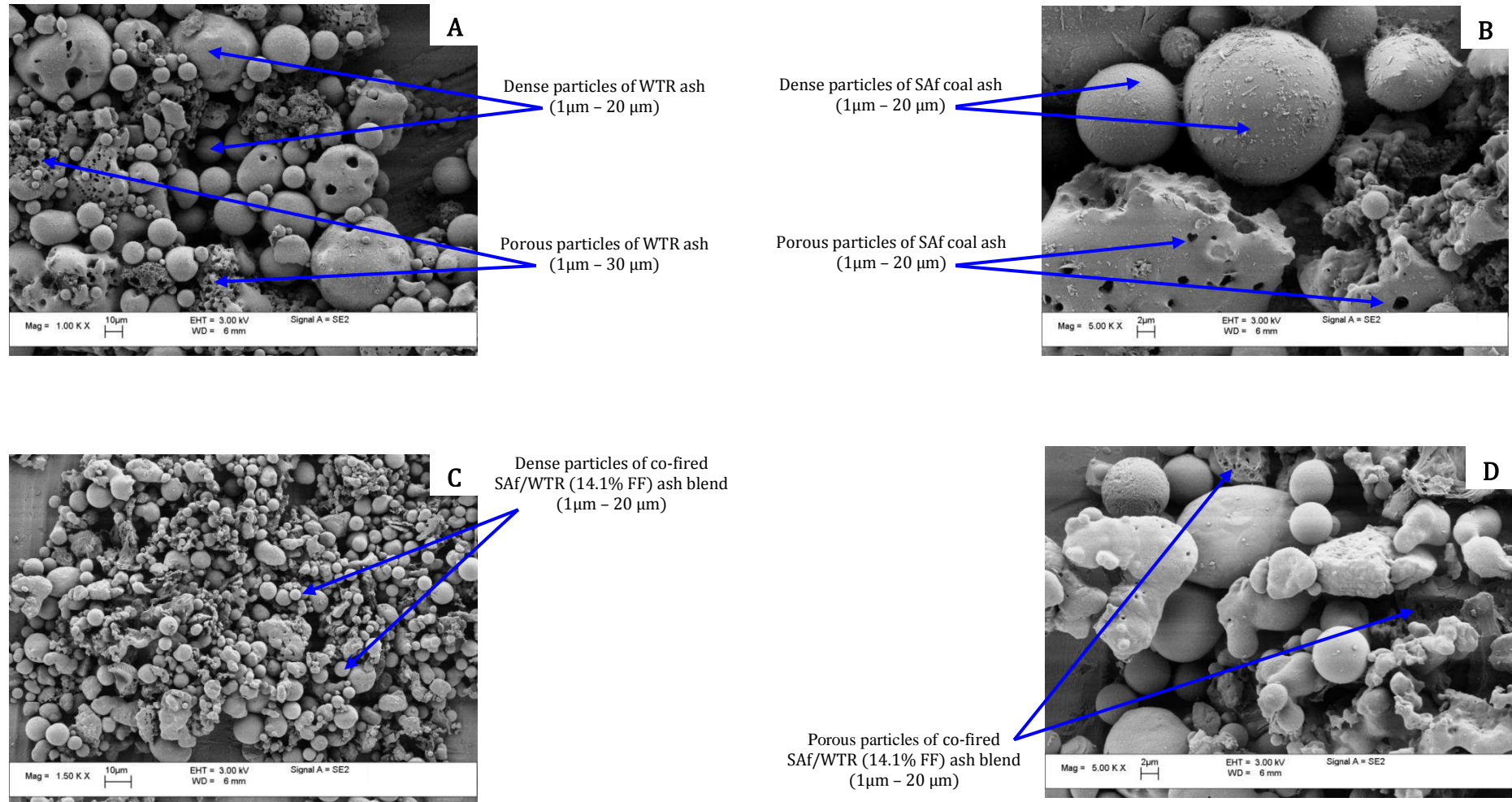
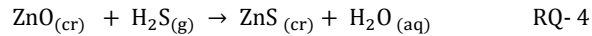


**Fig 6.** SEM images of fly ash collected from the cyclone trap of the 80 kW<sub>th</sub> CTF for the pure combustion of WTR (A), pure combustion of South African coal (B) and co-fired SAf/WTR (14.1% FF) ash blend (C, D).



The particle size distribution for pure fired SAF, WTR and co-fired SAF/WTR ashes as measured by the particle size analyser (Malvern Mastersizer 2000) range from  $\sim 1 \mu\text{m}$  to  $\sim 20 \mu\text{m}$  for the pure fired SAF, WTR and co-fired SAF/WTR ashes. This is supported by the SEM images of the pure fired SAF, WTR and co-fired SAF/WTR ashes (Fig 6A-D), which provide a scale of the particle images captured ( $\sim 1 \mu\text{m}$  to  $\sim 30 \mu\text{m}$ ). Therefore presenting further evidence to suggest that the Zn is bypassing the cyclone trap via the suggested sub-micron aerosol phase. The SEM images of the pure fired SAF, WTR and co-fired SAF/WTR (14.1% FF) reveal a range of dense and porous ash particles as shown by Fig 6A-D.

ZnO is not a component that is typically associated with coal ashes, from which the fusibility correlations (Table 1) have been derived. However previous studies[49, 50] have shown the desulphurisation potential of ZnO in removal of hydrogen sulphide ( $\text{H}_2\text{S}$ ) from industrial processes (natural gas processing, petroleum refining, petrochemical plants, coke ovens and coal gasifiers). The use of ZnO in the removal of  $\text{H}_2\text{S}$  demonstrates its basic properties, as presented below by RQ-4 [50].



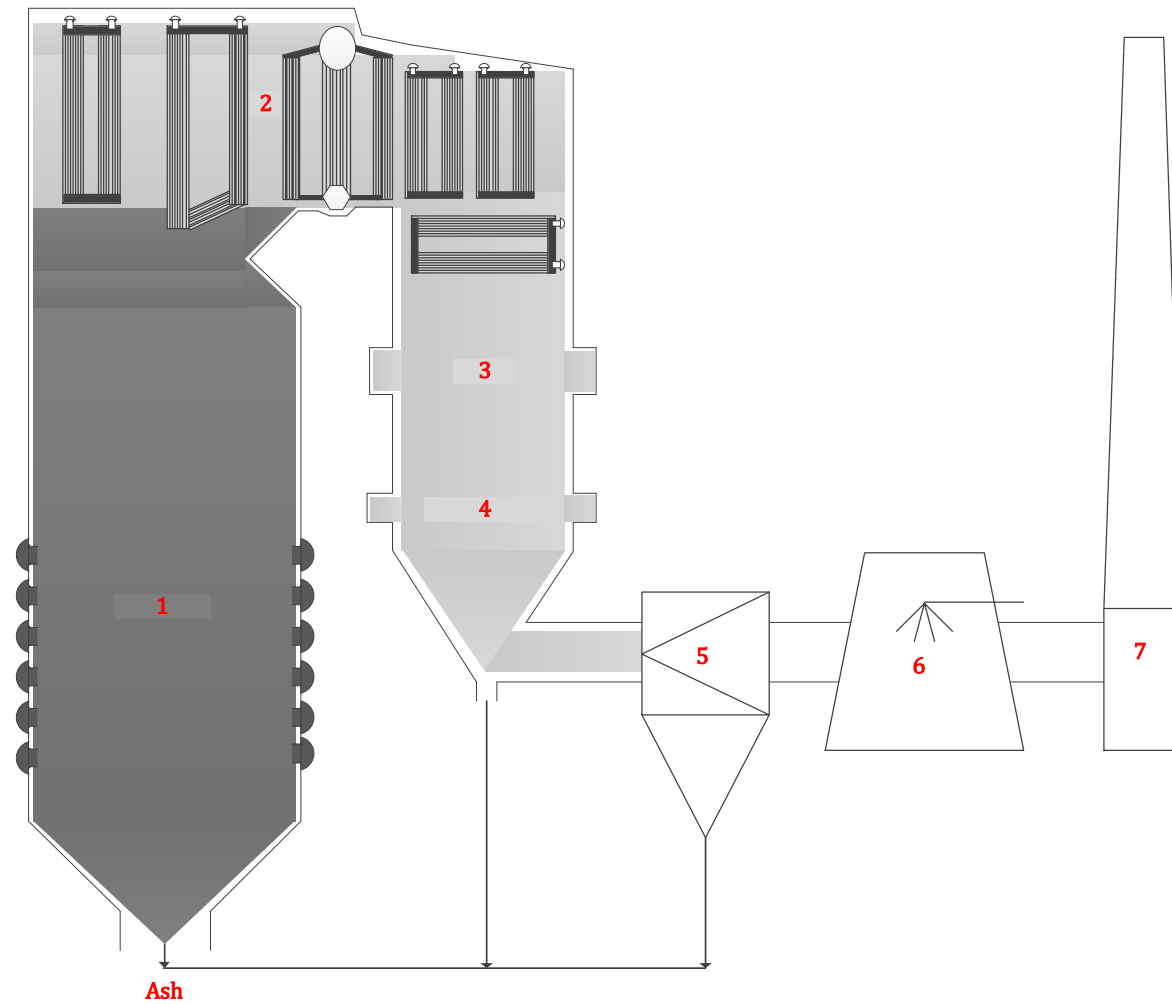
cr = crystalline, g = gas, and aq = aqueous solution

Therefore, it is reasonable to suggest that ZnO would enter the numerator of the modified version of the B/A ratio (EQ-1), as demonstrated below:

$$\frac{(B + \text{ZnO})}{A} = \frac{\text{Fe}_2\text{O}_3 + \text{CaO} + \text{Na}_2\text{O} + \text{K}_2\text{O} + \text{MgO} + \text{ZnO}^*}{\text{SiO}_2 + \text{Al}_2\text{O}_3 + \text{TiO}_2}$$

It is predicted that ZnO will not contribute to in-furnace slagging, due to ZnO volatilising to form a Zn vapour ( $>1200 \text{ }^\circ\text{C}$ ) equivalent to position 1 (Fig 7). Zn vapour is likely to be entrained with the flue gas through the combustion chamber. Therefore the Zn is not subjected to partial melting to form slag ( $\text{SiO}_2$ ,  $\text{Al}_2\text{O}_3$ ,  $\text{Fe}_2\text{O}_3$ ,  $\text{CaO}$ ,  $\text{MgO}$ ,  $\text{Na}_2\text{O}$ ,  $\text{TiO}_2$  and  $\text{K}_2\text{O}$ ) within the furnace or concentrate significantly within bottom ash. This is further supported by the experimental evidence of the present study and historical literature [36-41, 46 and 47]. ZnO is also perceived to be a low fouling risk as experimental XRF/ICP-OES analysis detected insignificant levels of ZnO within the fly ash and deposits collected from the cooled post combustion surfaces of the CTF equivalent to position 2 (Fig 7). If Zn is remaining in a suspended aerosol form it is further suggested that capture by the ash filtration system (Fig 7, position 5) and flue gas scrubbing unit (Fig 7, position 6). The temperatures at position 5 and 6 are sufficiently low for the vapour phase Zn to reform as crystalline  $\text{ZnO} \rightleftharpoons \text{ZnSO}_4$  (RQ-3). The technologies denoted by position 5 and 6 (Fig 7) have effectively demonstrated high efficiencies of trace metal removal from flue gases emanating from PF furnaces [41, 47].

**Fig 7.** Potential combustion and post combustion behaviour of ZnO/Zn for pure fired WTR and co-fired fuel blends of SAF/WTR within a PF boiler. 1= in-furnace, 2= convective heat exchange surfaces super-heaters/re-heaters, 3=SCR, 4=Air heater, 5=Ash filtration (ESP/Bag-house), 6= Flue gas scrubber (FGD), 7=Flue stack.



## 4. Conclusions

In this study a range of pure fired bituminous coal ashes, biomass ash, pure fired WTR ash and co-fired SAF/WTR fuel blends were characterised in accordance to their respective mineral matter (metal oxides) constituents. An assessment of the deposition behaviour for slagging and fouling was calculated by use of fusibility correlations.

Ash derived from the pure firing of WTR and co-fired SAF/WTR fuel blends showed minimal risk of slagging and fouling in accordance to the fusibility correlations employed. The Zn in the form of ZnO present within WTR ash was observed to be significant, however the ashes collected from the 80 kW<sub>th</sub> CTF showed lower levels of Zn than anticipated for pure fired WTR and the co-fired SAF/WTR fuel blends. It was experimentally observed that Zn enrichment was not significant within the fly ash collected by the cyclone trap or deposits on the cooler post-combustion sections of the CTF. This suggests that the Zn may well be forming a submicron aerosol, based on the behaviour of trace metals within a furnace. It is suggested that ZnO will not contribute to in-furnace slagging, due to ZnO volatilising to Zn forming a vapour aerosol able to pass through the combustion chamber. ZnO is also perceived to be a low fouling risk as insignificant levels were detected within the fly ash and deposits collected from the cooled post combustion surfaces of the CTF. Based on the fusibility correlations it is believed that the introduction of WTR as a secondary fuel will not alter the deposition behaviour of the ash presenting a low risk of slagging and fouling within coal fired power plants. This study has identified that further experimental work is required in order to characterise the physicochemical properties of ZnO. Nonetheless this initial investigation of WTR ash and co-fired SAF/WTR ash is a direct response in addressing the potential use of WTR as a secondary fuel within coal fired boilers.

## Acknowledgments

We would like to thank the UK EPSRC for a research grant (No. EP/D502020/1) and Dr. William Livingston of Doosan Power Systems, for the mineral matter analysis of the respective raw South African coal, raw waste tyre and post combusted South African coal/waste tyre fuel ashes.

## Appendix

The theoretical mass balance for the ZnO weight percentage (wt%) as summarised by Table 5 was determined firstly by calculating the mass flow rates of the primary fuel SAF (South African coal) and the secondary fuel WTR (waste tyre rubber) along with their subsequent fuel blends (EQ-1 to EQ-3). This was then followed by determining the contribution of ash from the SAF, WTR and the respective SAF/WTR fuel blends (EQ-4 to EQ-5). The theoretical content of ZnO wt% present within the fuel blends and the resultant ash blends of SAF/WTR was then calculated and is expressed by EQ-4 to EQ-8.

Let  $\dot{m}_{SAF}$  denote the mass flow rate (kg/hr) of SAF, FF(%) the thermal input of the SAF,  $Q_{CTF}$  the thermal rating (80 kW) of the CTF and  $CV_{SAF}$  the gross calorific value (MJ/kg) of SAF coal.

$$\dot{m}_{SAF} = \left( \left( 1 - \left( \frac{FF(\%)}{100} \right) \right) \times \left( \frac{Q_{CTF}}{CV_{SAF} \times \left( \frac{1000}{3600} \right)} \right) \right) \quad [EQ - A1]$$

The secondary fuel mass flow rate (kg/hr) as denoted by  $\dot{m}_{WTR}$  for any given FF(%) thermal input of WTR was calculating in the exact same way as EQ-1.0, where  $CV_{SAF}$  in EQ-1 was substituted by  $CV_{WTR}$  representing the gross calorific value (MJ/kg) of WTR.

$$\dot{m}_{WTR} = \left( \left( 1 - \left( \frac{FF(\%)}{100} \right) \right) \times \left( \frac{Q_{CTF}}{CV_{WTR} \times \left( \frac{1000}{3600} \right)} \right) \right) \quad [EQ - A2]$$

Therefore the total mass flow rate (kg/hr) for any SAF/WTR fuel blend ( $\dot{m}_{SAF/WTR}$ ) is calculated as follows.

$$\dot{m}_{SAF/WTR} = (\dot{m}_{SAF} + \dot{m}_{WTR}) \quad [EQ - A3]$$

The mass flow rate (kg/hr) of the ash blend ( $\dot{m}_{Ash, Saf/WTR}$ ) is determined by knowing the respective mass flow rates of the SAF and WTR (EQ-1 to EQ-2). The  $Ash(\%)_{SAf,WTR}$  represents the respective ash contents of SAF and WTR (Table 2).

$$\dot{m}_{Ash, Saf/WTR} = (\dot{m}_{SAf} \times Ash(\%)_{SAf}) + (\dot{m}_{WTR} \times Ash(\%)_{SAf}) \quad [EQ - A4]$$

The mass fraction of the ash blend (EQ-4) with respect to any given SAF/WTR fuel blend (EQ-3) yields the percentage ash blend ( $Ash_{SAf/WTR}(\%)$ ) as presented by EQ-5.

$$Ash_{SAf/WTR}(\%) = \left( \left( \frac{\dot{m}_{Ash, Saf/WTR}}{\dot{m}_{SAf/WTR}} \right) \times 100 \right) \quad [EQ - A5]$$

Therefore the mass flow rate (kg/hr) of zinc oxide (ZnO) for any given fuel blend is denoted as  $\dot{m}_{ZnO, Saf/WTR}$  and is determined by knowing the total mass flow rate (kg/hr) ( $\dot{m}_{SAf/WTR}$ ) for any SAF/WTR fuel blend (EQ-1 to EQ-3). The  $ZnO(wt\%)_{SAf,WTR}$  represents the wt% of zinc oxide within the SAF and WTR (Table 2).

$$\dot{m}_{ZnO\ SAf/WTR} = (\dot{m}_{SAf} \times ZnO(\%)_{SAf}) + (\dot{m}_{WTR} \times ZnO(\%)_{WTR}) \quad [EQ - A6]$$

Therefore the theoretical wt% fraction that ZnO represents for any SAF/WTR fuel blend is further presented by EQ-7, and is denoted by  $ZnO_{SAf/WTR}(\%)$ . Let  $\dot{m}_{ZnO\ SAf/WTR}$  denote the mass flow rate (kg/hr) of ZnO for any SAF/WTR fuel blend (EQ-6) and  $\dot{m}_{SAf/WTR}$  the total mass flow rate (kg/hr) for any SAF/WTR fuel blend (EQ-3).

$$ZnO_{SAf/WTR}(\%) = \left( \left( \frac{\dot{m}_{ZnO\ SAf/WTR}}{\dot{m}_{SAf/WTR}} \right) \times 100 \right) \quad [EQ - A7]$$

Thus the theoretical ZnO wt% that is concentrated within the ash SAF/WTR blend can be determined and is presented by EQ-8. Let  $ZnO_{SAf/WTR}(\%)$  denote the fraction of ZnO for any SAF/WTR fuel blend (EQ-7) and  $Ash_{SAf/WTR}(\%)$  as the percentage ash blend (EQ-5).

$$\begin{aligned} & \textit{Theoretical} \\ ZnO_{Ash, Saf/WTR}(\%) &= ZnO_{SAf/WTR}(\%) \times Ash_{SAf/WTR}(\%) \end{aligned} \quad [EQ - A8]$$

## References

1. Elbaba IF, Wu C, Williams PT. Hydrogen production from the pyrolysis gasification of waste tyres with a nickel/cerium catalyst. *International Journal of Hydrogen Energy* 2011;36:6628-37.
2. Ko DCK, Mui ELK, Lau ST, McKay G. Production of activated carbons from waste tire – process design and economical analysis. *Waste Manage* 2004;24(9):875–88.
3. Muneer T, Asif M, Munawwar S. Energy supply, its demand and security issues for developed and emerging economies, *Renew Sustain. Energy Rev* 2005;9(5):444–73.
4. Webb AH, Hunter GC. Power-station contributions to local concentrations of NO<sub>2</sub> at ground level. *Environ Pollut* 1998;102:283–8.
5. Pudasainee D, Sapkota B, Shrestha ML, Kaga A, Kondo A, Inoue Y. Ground level ozone concentrations and its association with NO<sub>x</sub> and meteorological parameters in Kathmandu Valley. *Nepal Atmos Environ* 2006;40(40):8081–7.
6. Normann F, Andersson F, Leckner B, Johnsson F. High-temperature reduction of nitrogen oxides in oxy-fuel combustion, *Fuel*, 2008;87:3579-585.
7. Nimmo W, Singh S, Gibbs BM, Williams PT. The evaluation of waste tyre pulverised Fuel for NO<sub>x</sub> reduction by reburning. *Fuel* 2008;87:2893–900.
8. Singh S, Nimmo W, Gibbs BM, Williams PT. Waste tyre rubber as a secondary fuel for power plants *Fuel*. 2009;88:2473–480.
9. Singh S, Nimmo W, Javed MT, Williams PT. *Co-combustion of Pulverized Coal with Waste Plastic and Tire Rubber Powders*. *Energy & Fuels* 2011;25:108-118.
10. Alzueta MU, Glarborg P, DamJohansen K. Low temperature interactions between hydrocarbons and nitric oxide: an experimental study. *Combust Flame* 1997;109(1–2):25–36.
11. Bilbao R, Millera A, Alzueta MU, Prada L. Evaluation of the use of different hydrocarbon fuels for gas reburning. *Fuel* 1997;76(14–15):1401–7.
12. Laresgoiti MF, de Marco I, Torres A, Caballero B, Cabrero MA, Chomon MJ. Chromatographic analysis of the gases obtained in tyre pyrolysis. *J Anal Appl Pyrol* 2000;55(1):43–54.
13. Cunliffe AM, Williams PT. Composition of oils derived from the batch pyrolysis of tyres. *J Anal Appl Pyrol* 1998;44(2):131–52.
14. Linak WP, Wendt JOL. Toxic metal emissions from incineration: mechanisms and control, *Prog. Energy Combust. Sci.* 1993;19:145–85.

15. Kinoshita T, Yamaguchi K, Akita S, Nii S, Kawaizumi F, Takahashi K, Hydrometallurgical recovery of zinc from ashes of automobile tire wastes. *Chemosphere* 2005;59:1105-1111.
16. Aylón E, Murillo, Fernández-Colino A, Aranda A, García T, Callén MS, Mastral AM. Emissions from the combustion of gas-phase products at tyre pyrolysis. *J. Anal. Appl. Pyrolysis* 2007;79:210-214.
17. Reid WT. and Cohen P. The Flow Characteristics of Coal-Ash Slags in the Solidification Range, *Trans. ASME* 1944; 66: 685-690.
18. Reid WT. The Relation of Mineral composition to slagging, fouling and erosion during and after combustion. *Prog Energy Combust Sci* 1984;10:159-75.
19. Bryers RW. The Physical and Chemical Characteristics of Pyrites and Their Influence on Fireside Problems, *J. Engn Pwr* 1976;98:517-527.
20. Couch, G. Understanding slagging and fouling in PF combustion. IEA Coal Research; 1994.
21. Hatt RM. Fireside deposits in coal-fired utility boilers. *Prog. Energy Combust. Sci* 1990;16:235-241.
22. Nakabayashi Y. Yugami H. Iritani J. Haneda H. Namiki T. and Masuyama F. In 'Coatings and Bimetals for Aggressive Environments', Conference Proceedings, American Society of Mechanical Engineers; 1985.
23. ten Brink HM. Smart JP, Vleeskens JM and Williamson J. Flame transformations and burner slagging in a 2.5 MW furnace firing pulverized coal I. Flame transformations. *Fuel* 1994;73:11.
24. Bool LE, Peterson TW, Wendt JOL. The partitioning of iron during the combustion of pulverized coal. *Combust Flame* 1995;100:262-70.
25. Russell NV, Wigley F, Williamson J. The roles of lime and iron oxide on the formation of ash and deposits in PF combustion. *Fuel* 2002;81:673-681.
26. Bryers RW. Fireside slagging, fouling, and high-temperature corrosion of heat-transfer surface due to impurities in steam-raising fuels. *Progress in Energy and Combustion Science* 1996; 22:29-120.
27. Couch, G. R. Lignite upgrading. IEA Coal Research; 1990.
28. Pronobis M. The influence of biomass co-combustion on boiler fouling and efficiency. *Fuel* 2006;85:474-480.
29. Hsu LL, Kubarych KG, Stetson AR, Metcalfe AG. Mechanisms of fouling, slagging and corrosion by pulverised coal combustion. US Department of Energy, DOE/PC40272-8 (DE85008002);1984.

30. Skorupska NM. Coal specifications- impact on power station performance. IEA Coal Research; 1993.
31. Pronobis M. Evaluation of the influence of biomass co-combustion on boiler furnace slagging by means of fusibility correlations. *Biomass and Bioenergy* 2005;28:375–383.
32. Pedersen LS, Nielsen HP, Kiil S, Hansen AL, Dam-Johansen K, Kildsig F, Christensen J and Jespersen P. Full-scale co-firing of straw and coal. *Fuel* 1996;75:1584-90.
33. Heinzl T, Siegle V, Spliethoff H, Hien KRG. Investigation of slagging in pulverised fuel co-combustion of biomass and coal at a pilot-scale test facility. *Fuel Processing Technology* 1998;54:109-125.
34. Helble JJ, Srinivaschar S and Boni AA. Factors influencing the transformation of minerals during pulverised coal combustion. *Prog. Energy Combust. Sci* 1990;16:267-279.
35. Gupta, S.K. Gupta, R.P. Bryant G.W. and T.F. Wall The effect of potassium on the fusibility of coal ashes with high silica and alumina levels. *Fuel* 1998;77:1195-1201.
36. Frandsen F. Dam-Johansen K and Rasmussen P. Trace elements from coal combustion and gasification of coal-an Equilibrium approach. *Prog. Energy Combust. Sci.* 1994;20:115-138.
37. Clarke LB. The fate of trace elements during coal combustion and gasification: an overview. *Fuel* 1993;72:731-736.
38. Querol X, Fernandez TJL, Lopez SA. Trace elements in coal and their behaviour during combustion in a large station. *Fuel* 1995;74:331–343.
39. Haynes, B. S. Neville, M. Quann, R. J. Sarofim, A. F. Factors governing the surface enrichment of fly ash in volatile trace species, *J. Colloid Interface Sci.* 87;1982:266– 278.
40. Kramlich, J.C. Newton, G. H. Influence of coal rank and pretreatment on residual ash particle size, *Fuel Process. Technol.* 1994;37:143– 161.
41. Linak, W.P. Wendt, J.O.L. Trace metal transformation mechanisms during coal combustion, *Fuel Process. Technol.* 39;1994:173– 198.
42. Clarke LB. and Sloss LL. Trace Elements. IEA Coal Research; 1992.
43. Meij R. Tracking trace elements at a coal-fired power plant equipped with a wet flue-gas desulphurisation facility. Kema Scientific & Technical Reports; 1989.
44. Chadwick MJ, Highton NH and Lindman N. Environmental Impacts of Coal Mining and Utilization. Pergamon Press; 1987.

45. Germani MS and Zoller WH. Environ, Sci, Technol, 1988;22:1079.
46. Ratafia-Brown JA. Overview of trace elements partitioning in flames and furnaces of utility coal-fired boilers. Fuel Process. Technol 1994;39:139–157.
47. Xu M, Yan R, Zheng C, Qiao Y, Han J, Sheng C. Status of trace element emission in a coal combustion process: a review. Fuel Process. Technol 2003;85:215– 237.
48. Spliethoff H. Advanced Solid Fuel Conversion–Fundamentals, Technologies and Research Demand, Lehrstuhl für Energiesysteme TUM. The 9th International Conference on Energy for a Clean Environment (Clean Air); 2007.
49. Polychronopoulou K, Fierrob JLG, Efstathioua AM. Novel Zn–Ti-based mixed metal oxides for low-temperature adsorption of H<sub>2</sub>S from industrial gas streams. Applied Catalysis B: Environmental 2005;57:125–137.
50. Wang X, Sun T, Yang J, Zhao L, Jia J. Low-temperature H<sub>2</sub>S removal from gas streams with SBA-15 supported ZnO nanoparticles. Chemical Engineering Journal 2008;142:48–55.

